Journal of Molecular Structure: THEOCHEM 869 (2008) 1–5

Contents lists available at ScienceDirect

Journal of Molecular Structure: THEOCHEM

journal homepage: www.elsevier.com/locate/theochem

DFT calculations of the structure and electronic properties of late 3d transition metal atoms endohedrally doping C_{60}

Rubén E. Estrada-Salas *, Ariel A. Valladares

Departamento de Materia Condensada y Criogenia, Instituto de Investigaciones en Materiales, Universidad Nacional Autónoma de México, México D. F., C. P. 04510, Mexico

ARTICLE INFO

Article history:
Received 19 May 2008
Received in revised form 6 August 2008
Accepted 13 August 2008
Available online 29 August 2008

Keywords:
Endohedral metallofullerenes
DFT calculations
Metal-cage hybridization

ABSTRACT

Structural and electronic properties of M@C_{60} (M = Mn, Fe, Co, Ni, Cu or Zn) were studied via the density functional BPW91/DNP level of theory. Minimal energy structures for each endohedral metallofullerene were obtained. Hybridizations were found between the Mn, Fe, Co, and Ni 3d valence orbitals and the C_{60} cage orbitals, while none were found between the Cu and Zn orbitals and the C_{60} cage orbitals. These findings were obtained with the preferential position of the metal atom inside the fullerene cage. Mn@C_{60}, Fe@C_{60}, Co@C_{60}, and Cu@C_{60} endohedral metallofullerenes present a paramagnetic behavior.

1. Introduction

Metals encapsulated by fullerene cages (endohedral metallofullerenes) have attracted special attention as a new class of technologically relevant materials due to their combined fullerene-like and metallic properties [1]. This kind of fullerenes has potential applications in diverse fields ranging from medicine to electronics and quantum computing [1–5].

Contrary to expectation, the abundance of endohedral fullerenes obtained by conventional methods of fullerene synthesis (laser and arc vaporization) is higher than C_{60} and C_{70} [2] (e.g. $La_2@C_{80}$, $Sc_3@C_{84}$, etc.). However, it has been possible to obtain macroscopic amounts of C_{60}–based endofullerenes by other methods such as ion implantation [6]. Typically, the elements that can be trapped inside fullerenes are those within the groups 1–4, 15 and 18 of the periodic table [7].

To the best of our knowledge, there are only a few reports on the synthesis (or attempts to synthesize) and characterization of unconventional endofullerenes with late 3d transition metals (groups 7–12 of the periodic table) [7–18]. Also, recently some companies have started to produce and commercialize some of this new endohedral metallofullerenes [16–19]. However, more studies are needed to get a better understanding of their properties and hence to elucidate their potential applications. This is the motivation for performing the calculations presented in this letter.

2. Calculation details

Full geometry optimizations and total energy calculations were performed with the DFT-based program package DMol^3 [20,21] at the generalized gradient approximation (GGA) density functional BPW91 [22,23] level of theory with the double numerical atomic orbital basis set plus polarization functions (DNP). We choose the BPW91 functional because of its well tested good performance [24–27], and also because the large dimension of the systems makes the use of higher order theoretical approaches such as the second-order many-body perturbation method (MP2) or the configuration interaction (CI) method, unfeasible [28].

In order to find the preferential position of the metal atom inside the C_{60} cage, five initial positions were considered: (1) in the center of the cage, M@C_{60}^{c}; (2) on top of a hexagonal face, M@C_{60}^{h}; (3) on top of a pentagonal face, M@C_{60}^{p}; (4) on top of the bond sheared by two hexagonal faces, M@$C_{60}^{h/h}$; and (5) on top of the bond sheared by a pentagonal face and a hexagonal one, M@$C_{60}^{h/p}$. Full geometry optimization was performed for each of these five conformations and for each of the six endofullerenes.

Mulliken [29] and Hirshfeld [30] population analysis schemes have been used to determine the charge and spin states of the metal atoms located inside the C_{60} cage. Although Mulliken analysis is the most commonly used scheme, it has been found that it is strongly dependent on the basis set and may fail in describing charge distribution. Therefore, we also carried out Hirshfield analysis, which is almost completely insensitive to improvement of the basis set and yields chemically meaningful charges [31–33]. Our results show that both population analysis schemes predict almost the same charge and spin state for each endohedral atom.

* Corresponding author. Tel./fax: +52 55 5622 4636.
E-mail addresses: eduardo.estrada@correo.unam.mx, dr_jim_es@yahoo.com (R.E. Estrada-Salas), valladar@servidor.unam.mx (A.A. Valladares).

0166-1280/$ - see front matter © 2008 Elsevier B.V. All rights reserved.
doi:10.1016/j.theochem.2008.08.017

3. Results and discussions

3.1. Minimal energy structures

After full geometry optimization calculations, two stable conformations were found for $Mn@C_{60}$ and $Fe@C_{60}$: one with the metal atom on the center of the C_{60} cage ($M@C_{60}^{c}$), and the other with the metal atom on top of a hexagonal face ($M@C_{60}^{h}$). The energy of the $Mn@C_{60}^{c}$ conformation is 0.079 eV lower than the $Mn@C_{60}^{h}$ conformation, whereas the energy of the $Fe@C_{60}^{h}$ conformation is 0.88 eV lower than the $Fe@C_{60}^{c}$ conformation.

For $Cu@C_{60}$ and $Zn@C_{60}$ only the conformation with the metal atom located at the center of the C_{60} cage was stable ($M@C_{60}^{c}$). However, for $Co@C_{60}$ and $Ni@C_{60}$ the five conformations considered were stable.

In order to probe that the stable conformations found for each endofullerene are true minimal energy structures, harmonic vibrational frequencies were calculated [34]. For $Mn@C_{60}$ and $Fe@C_{60}$ only the $M@C_{60}^{h}$ conformation showed to be a true minimal energy structure, because all its vibrational frequencies have real values. The $M@C_{60}^{c}$ conformation showed two imaginary vibrational frequencies, so it is not a true minimum but rather a second order saddle point on the molecular potential energy surface.

For $Cu@C_{60}$ and $Zn@C_{60}$ the unique stable conformation found with the metal atom located at the center of the C_{60} cage ($M@C_{60}^{c}$), is also a true minimal energy structure. In the case of $Co@C_{60}$ and $Ni@C_{60}$, two conformations showed to be true minimal energy structures: one with the metal atom on top of a hexagonal face ($M@C_{60}^{h}$), and the other with the metal atom on top of a pentagonal face ($M@C_{60}^{p}$). The energy of the $Co@C_{60}^{h}$ conformation is 0.31 eV lower than the $Co@C_{60}^{p}$ conformation, whereas the energy of the $Ni@C_{60}^{p}$ conformation is 0.095 eV lower than the $Ni@C_{60}^{h}$ conformation.

We found a Fe–C distance of 2.058 Å for the minimal energy structure of the $Fe@C_{60}$ molecule, which is in agreement with Pradeep et al. [11] who found a Fe–C distance of 2.06 Å by EXAFS measurements. Theoretical calculations by Kowalska et al. [35] and Tang et al. [36] using semiempirical and DFT methods, respectively, also found that the minimal energy structure of the $Fe@C_{60}$ molecule is that with the Fe atom on top of a hexagonal face of the C_{60} cage. On the other hand, our finding that the Cu atom is located in the center of the cage seems to be in disagreement with the ESR measurements of Knapp et al. [8], who found that the encased copper atom occupies a well-defined off-center position even at room temperature. However, Elliot et al. [9], after a better characterization, say that the compound synthesized by Knapp et al., may not really be the endohedral metallofullerene $Cu@C_{60}$ but a Cu(II) dithiocarbamate.

DFT molecular dynamics simulations [37], at VWN/DNP level of theory [38], were carried out to verify the stability of endohedral metallofullerenes studied at room temperature. All dynamics simulations started with the metal atom at the center of the fullerene cage.

While Mn and Fe atoms moved from the center towards one hexagonal face and then bonded to this face, Cu and Zn atoms only moved around the center but did not bond to any face. These simulations indicate that the minimal energy structures found for these four endofullerenes are also the most stable conformations at room temperature.

In the cases of $Co@C_{60}$ and $Ni@C_{60}$, molecular dynamics simulations show that both Co and Ni atoms are freely moving around the fullerene wall inside the cage at room temperature. This may explain why we found that the five conformations considered were stable for both of these endofullerenes.

3.2. Electronic properties

In Table 1 we present the results obtained for the Mulliken and the Hirshfeld population analysis. Both analysis schemes were calculated for the minimal energy structure of each endofullerene. For $Co@C_{60}$ and $Ni@C_{60}$ two sets of results are presented: one set for the structure with the metal atom on top of a hexagonal face ($M@C_{60}^{h}$), and another set for the structure with the metal atom on top of a pentagonal face ($M@C_{60}^{p}$).

Both analyses find that there is charge transfer from the Mn, Fe, Co or Ni atom to the fullerene cage. In these four cases, the charge transfer amount is less than unity, which is in agreement with the Mössbauer measurements of Pradeep et al. [11], who found a near-zero oxidation state for iron inside C_{60}.

In the cases of $Cu@C_{60}$ and $Zn@C_{60}$, although the Hirshfeld analysis finds a slight charge transfer from the metal atom to C_{60} cage, the Mulliken analysis finds the inverse situation: a slight charge transfer from the fullerene cage to the Cu or Zn atom. Nevertheless, because these are very small values, it seems that in fact there is no charge transfer from the Cu or Zn atom to the C_{60} molecule. This seems to be in disagreement with the ESR measurements of Huang et al. [7] and Knapp et al. [8], who found that Cu must be in its oxidation state of 2+ ($3d^9$), after transferring two electrons to the C_{60} cage. But, as we said above, Elliot et al. [9] say that the compound synthesized by Huang et al. and Knapp et al. may not really be $Cu@C_{60}$ but a Cu(II) dithiocarbamate, and this may explain the disagreement between our results and theirs.

The Mulliken analysis also finds intra-atomic charge transfer from 4s to 3d within the Mn, Fe, Co and Ni atoms. For the case of $Fe@C_{60}$, this is in agreement with theoretical calculations by Tang et al. [36]. In the case of Cu and Zn atoms the intra-atomic charge transfer is less appreciable than in the former cases and we can observe that Cu and Zn 3d and 4s shells remain almost completely filled.

The molecules $Mn@C_{60}$, $Fe@C_{60}$, $Co@C_{60}$ and $Cu@C_{60}$ have no zero net spin population and therefore these endohedral metallofullerenes could display a paramagnetic behavior. According to the Mulliken analysis, in $Mn@C_{60}$, $Fe@C_{60}$ and $Co@C_{60}$ the unpaired spins are located in the 3d shell of the metal atoms, whereas in $Cu@C_{60}$ the unpaired spin corresponds to the 4s orbital. Both population analysis schemes show that $Mn@C_{60}$, $Co@C_{60}$ and $Cu@C_{60}$ are in a doublet spin state, while $Fe@C_{60}$ is in a triplet spin state. The paramagnetic behavior found for $Fe@C_{60}$ is in agreement with experimental results of Pradeep et al. [11].

The spin states found for $Mn@C_{60}$ and $Fe@C_{60}$ are in agreement with the theoretical work of Lu et al. [39] despite the fact that they placed the metal atom in the center of the C_{60} cage to keep the I_h symmetry. Also, we can observe from our results, that charge and spin states of $Co@C_{60}$ and $Ni@C_{60}$ are practically independent of the position of the metal atom inside the C_{60} cage. Unexpectedly, these findings seem to disagree with the assertion of Lu et al. [40] who say that the electronic properties of metallofullerenes may change dramatically with different arrangements of the metal atom inside the fullerene cage.

Due to this apparent conflict between our results and the experimental measurements of Huang et al. [7] and Knapp et al. [8], we perform geometry optimization calculations as well as Mulliken population analysis for $Cu@C_{60}$ molecule using another well tested density functional: the BLYP [24] functional with the DNP basis set. Preliminary results indicate that among the $Cu@C_{60}^{h}$, $Cu@C_{60}^{p}$ and $Cu@C_{60}^{c}$ structures, just the $Cu@C_{60}^{c}$ structure was stable after the geometry optimization calculations, showing that it is the unique minimum on the molecular potential energy surface. The performed Mulliken analysis at the BLYP/DNP level of theory for the $Cu@C_{60}^{c}$ molecule shows that Cu atom has almost zero net charge (0.045) and it also has one unpaired electron in the 4s orbital.

Table 1
Mulliken (M) and Hirshfeld (H) charges and spin populations calculated for the minimal energy structure of each endohedral metallofullerene at the BPW91/DNP level of theory

Orbitals in metal atom	$Mn@C_{60}^{h}$			$Fe@C_{60}^{h}$			$Co@C_{60}^{h}$			$Co@C_{60}^{p}$		
	Spin up	Spin down	Net spin	Spin up	Spin down	Net spin	Spin up	Spin down	Net spin	Spin up	Spin down	Net spin
4s	0.12	0.11	0.01	0.12	0.10	0.02	0.12	0.11	0.01	0.12	0.12	0.01
3d	3.47	2.60	0.87	4.53	2.47	2.06	4.67	3.40	1.26	4.50	3.61	0.89
4p	0.17	0.14	0.03	0.18	0.12	0.06	0.18	0.14	0.04	0.16	0.14	0.03
Total	ChargeM/H		SpinM/H	ChargeM/H		SpinM/H	ChargeM/H		SpinM/H	ChargeM/H		SpinM/H
Metal atom	0.35/0.24		0.90/0.84	0.47/0.23		2.13/2.03	0.34/0.22		1.31/1.28	0.33/0.21		0.92/0.90
Fullerene cage	−0.35/−0.25		0.10/0.17	−0.47/-0.23		−0.12/−0.03	−0.34/-0.22		−0.32/−0.28	−0.32/−0.21		0.08/0.10
Endohedral complex	0.00/−0.01		1.0/1.01	0.00/0.00		2.01/2.00	0.00/0.00		0.99/1.00	0.01/0.00		1.00/1.00
Orbitals in metal atom	$Ni@C_{60}^{h}$			$Ni@C_{60}^{p}$			$Cu@C_{60}^{c}$			$Zn@C_{60}^{c}$		
	Spin up	Spin down	Net spin	Spin up	Spin down	Net spin	Spin up	Spin down	Net spin	Spin up	Spin down	Spin up
4s	0.11	0.11	0.0	0.11	0.11	0.00	1.00	0.02	0.98	0.99	0.99	0.00
3d	4.53	4.53	0.0	4.54	4.54	0.00	4.99	4.98	0.01	5.0	5.0	0.00
4p	0.14	0.14	0.0	0.12	0.12	0.00	0.03	0.02	0.01	0.04	0.04	0.00
Total	ChargeM/H		SpinM/H	ChargeM/H		SpinM/H	ChargeM/H		SpinM/H	ChargeM/H		SpinM/H
Metal atom	0.44/0.18		0.00/0.00	0.45/0.20		0.00/0.00	−0.06/0.11		1.0/0.67	−0.05/0.12		0.00/0.00
Fullerene cage	−0.44/−0.18		0.00/0.00	−0.46/−0.2		0.00/0.00	0.06/−0.11		0.00/0.33	0.06/−0.13		0.00/0.00
Endohedral complex	0.00/0.00		0.00/0.00	−0.01/0.00		0.00/0.00	0.00/0.00		1.00/1.00	0.01/−0.01		0.00/0.00

These findings agree with our calculations performed at the BPW91/DNP level of theory.

The Kohn–Sham electronic levels of the most stable $M@C_{60}$ structures obtained at the BPW91/DNP level together with those of pristine C_{60} are shown in Fig. 1. We can observe that there is no hybridization between Cu and Zn atomic orbitals and the C_{60} cage orbitals, with the Cu 3d (H_g) and 4s (A_g) levels and Zn 4s (A_g) level lying in the middle of the C_{60} HOMO–LUMO gap. The HOMO derived from the Cu and Zn 4s (A_g) orbital has no contribution to C_{60}, Fig. 2. On the other hand, the LUMO's of $Cu@C_{60}$ and $Zn@C_{60}$ are mainly derived from the C_{60} T_{1u} orbitals. The lack of hybridization between C_{60} orbitals and the endoatom orbitals has been found in other endohedral complexes, where the most stable structure has the guest atom situated in the center of C_{60} cage [28,41,42].

We can observe that Mn, Fe, Co and Ni atoms generate a number of allowed electronic levels in the middle of the C_{60} HOMO–LUMO gap, Fig. 1. Also, Mn, Fe, Co and Ni atoms cause the splitting of the threefold degenerate LUMO of C_{60} into a lower non-degenerate level (A_1) and an upper twofold degenerate level (3E), except

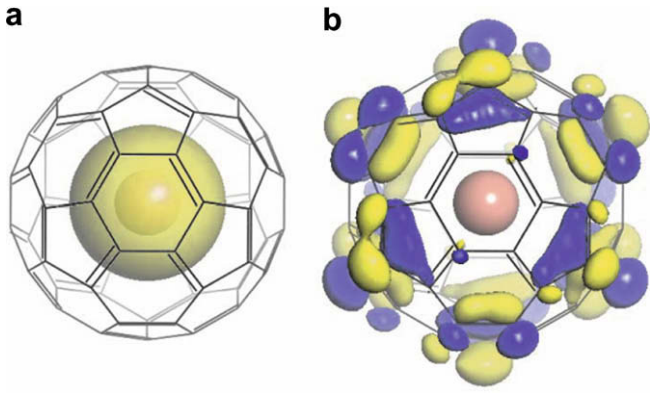

Fig. 2. Isosurfaces (the isovalue is 0.03 a.u.) of: (a) HOMO and (b) LUMO in the $Cu@C_{60}^{c}$ molecule. Blue and yellow indicate the positive and negative sign of the wavefunction, respectively. The $Zn@C_{60}^{c}$ molecule shows practically the same spatial representation of its HOMO and LUMO. (For interpretation of the references to colour in this figure legend, the reader is referred to the web version of this article.)

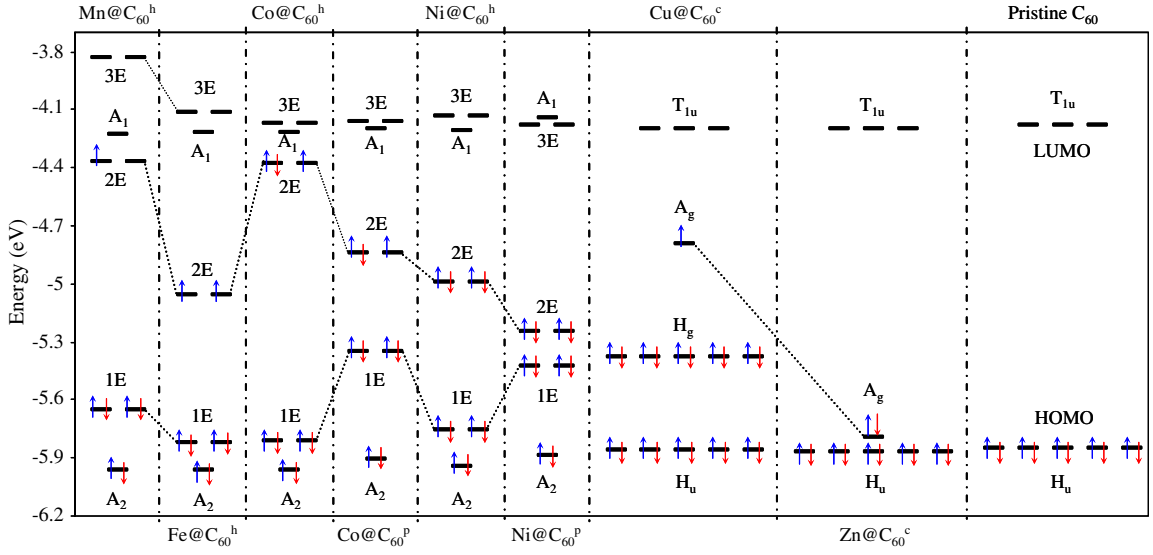

Fig. 1. Kohn–Sham electronic levels of the six studied endohedral metallofullerenes and HOMO–LUMO levels of pristine C_{60}, as predicted at the BPW91/DNP level of theory. It should be noted that there exist differences between the up- and down-spin energies, however, these differences are not illustrated in this diagram for simplicity.

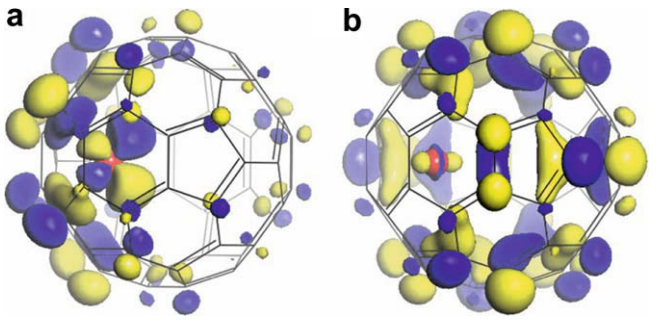

Fig. 3. Isosurfaces (the isovalue is 0.03 a.u.) of: (a) HOMO and (b) LUMO in the $Fe@C_{60}^{h}$ molecule. Blue and yellow indicate the positive and negative sign of the wavefunction, respectively. $Mn@C_{60}^{h}$, $Co@C_{60}^{h}$ and $Ni@C_{60}^{h}$ molecules show similar spatial representation of their HOMO and LUMO. (For interpretation of the references to colour in this figure legend, the reader is referred to the web version of this article.)

when Ni atom is on top of a pentagonal face. In this case the LUMO of C_{60} is split into an upper non-degenerate level (A_1) and a lower twofold degenerate level (3E). A similar splitting of the threefold degenerate LUMO of C_{60} has been observed in the interaction of C_{60} with alkali metals [43,44], and lanthanides [40,45]. The HOMO and LUMO of $Mn@C_{60}^{h}$, $Fe@C_{60}^{h}$, $Co@C_{60}^{h}$ and $Ni@C_{60}^{h}$, Fig. 3, show a clear mixing between the T_{1u} orbitals of the C_{60} and the 3d orbitals of the transition metal atoms. The same can be observed for $Co@C_{60}^{p}$ and $Ni@C_{60}^{p}$ molecules, Fig. 4. The orbital hybridization between the guest transition metal atoms and fullerene is a common characteristic in metallofullerenes [40,46–49].

In order to get a better understanding on the relationship between geometry and electronic structure we show in Fig. 5 the electron density in a plane containing the endoatom. For $Mn@C_{60}$, $Fe@C_{60}$, $Co@C_{60}$ and $Ni@C_{60}$ molecules, Fig. 5(a), we can observe a small electron accumulation between the endoatom and C_{60}. Therefore, the interaction of the Mn, Fe, Co and Ni endoatoms with C_{60} presents a small covalent character and, due to the small charge transfer found (table 1), it may also present a small ionic character. Similar behavior has been observed in the endohedral metallofullerene $Gd@C_{60}$ [40]. On the other hand, for $Cu@C_{60}$ and $Zn@C_{60}$ molecules, Fig. 5(b), there is practically no electron accumulation between the endoatom and C_{60}. Then, the interaction of Cu and Zn endoatoms with C_{60} is not covalent. However, as no charge transfer was found, it can not be ionic either. Similar behavior has been observed in the endohedral metallofullerene $Po@C_{60}$ [42].

In Table 2, we report the total energies (E_T), binding energies (E_b), energies of HOMO and LUMO, and energy gaps (E_g) of the endohedral metallofullerenes studied and pristine C_{60}. E_b is defined as the absolute value of the difference between the total energy of the molecule and the energy sum of the free atoms constituting the molecule, which is the usual standard for estimating the thermodynamic stability of a molecule [36]. $Mn@C_{60}$, $Cu@C_{60}$, and $Zn@C_{60}$ molecules have an E_b lower than the pristine C_{60}, while $Fe@C_{60}$, $Co@C_{60}$ and $Ni@C_{60}$ molecules have an E_b slightly higher than pristine C_{60}, however all metallofullerenes seem to have almost the same stability than the pristine fullerene.

A reduction of the gap can be observed for all of the endofullerenes with respect to pristine C_{60}, due to the electronic levels introduced by the metal atoms. In the case of $Mn@C_{60}$ and $Co@C_{60}^{h}$, the

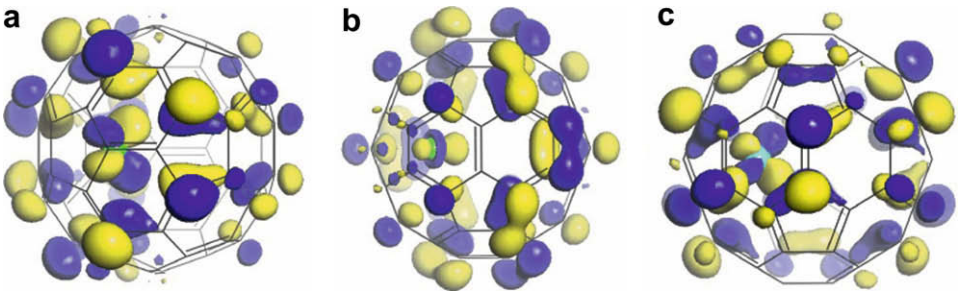

Fig. 4. Isosurfaces (the isovalue is 0.03 a.u.) of: (a) HOMO in the $Co@C_{60}^{p}$ and $Ni@C_{60}^{p}$ molecules; and (b, c) LUMO in the $Co@C_{60}^{p}$ and $Ni@C_{60}^{p}$ molecules, respectively. Blue and yellow indicate the positive and negative sign of the wavefunction, respectively. (For interpretation of the references to colour in this figure legend, the reader is referred to the web version of this article.)

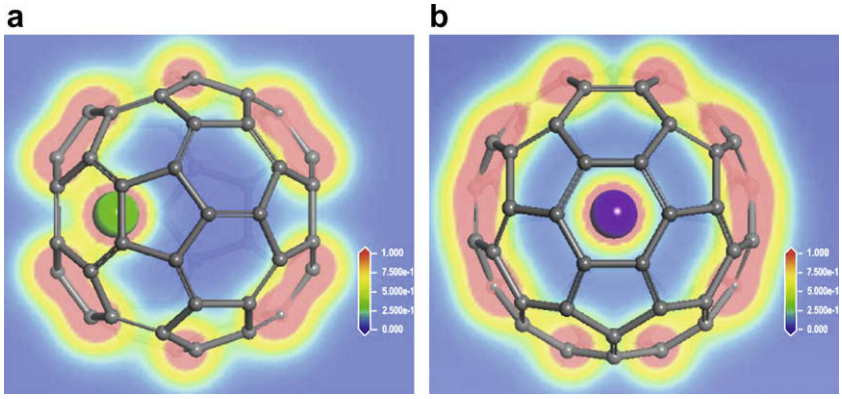

Fig. 5. Contour maps representing the electron density in a plane passing through the endoatom. The colors represent the value of the electron density: red stands for the maximum value while blue stands for the minimum value. (a) Contour map for $Co@C_{60}^{h}$ molecule. $Mn@C_{60}^{h}$, $Fe@C_{60}^{h}$, $Co@C_{60}^{p}$, $Ni@C_{60}^{h}$ and $Ni@C_{60}^{h}$ molecules show similar contour maps. (b) Contour map for $Zn@C_{60}^{c}$ molecule. $Cu@C_{60}^{c}$ molecule shows a similar contour map. (For interpretation of the references to colour in this figure legend, the reader is referred to the web version of this article.)

Table 2
Total energies (E_T), binding energies (E_b), and HOMO–LUMO gaps (E_g), in eV, of the six endohedral metallofullerenes studied and pristine C_{60}, as predicted at the BPW91/DNP level of theory

Fullerene	Total energy (E_T)	Binding energy (E_b)	HOMO	LUMO	Energy gap (E_g)	
					Calc.	Exp.
$Mn@C_{60}^{h}$	−93,548.218	441.274	−4.366	−4.228	0.138	–
$Fe@C_{60}^{h}$	−96,616.497	442.922	−5.062	−4.217	0.845	–
$Co@C_{60}^{h}$	−99,856.806	443.346	−4.382	−4.223	0.159	–
$Co@C_{60}^{p}$	−99,856.554	443.093	−4.844	−4.178	0.666	–
$Ni@C_{60}^{h}$	−103,274.007	443.624	−4.992	−4.207	0.785	–
$Ni@C_{60}^{p}$	−103,274.133	443.749	−5.249	−4.171	1.078	–
$Cu@C_{60}^{c}$	−106,871.802	441.274	−4.790	−4.202	0.588	–
$Zn@C_{60}^{c}$	−10,651.437	441.119	−5.795	−4.201	1.594	–
C_{60}	−62,225.413	441.564	−5.853	−4.179	1.674	1.65[a]

[a] From Ref. [50].

reduction of the gap is surprisingly large, while in the case of $Zn@C_{60}$ the reduction of the gap is minimal. For $Fe@C_{60}$, $Ni@C_{60}$ and $Cu@C_{60}$ molecules, the gap is also notably reduced. These results indicate an increase in the chemical reactivity of the fullerene by endohedral doping with late 3d transition metals.

4. Summary

We have studied the structural and electronic properties of late 3d transition metal atoms endohedrally doping C_{60} using the density functional BPW91 with the DNP basis set. We found that the most stable structure of $Mn@C_{60}$ and $Fe@C_{60}$ has the endoatom on top of a hexagonal face, whereas Cu and Zn atoms are situated in the center of C_{60} cage. On the other hand, $Co@C_{60}$ and $Ni@C_{60}$ show two stable structures: one with the metal atom on top of a hexagonal face and the other with the metal atom on top of a pentagonal face.

Mulliken and Hirshfeld population analysis show a near-zero oxidation state for all of the transition metal atoms used to dope C_{60}. The molecules $Mn@C_{60}$, $Fe@C_{60}$, $Co@C_{60}$ and $Cu@C_{60}$ present unpaired spins and therefore they should present a paramagnetic behavior.

The HOMO and LUMO of $Cu@C_{60}$ and $Zn@C_{60}$ indicate that there is no hybridization between the C_{60} orbitals and the endoatom orbitals, while the HOMO and LUMO of $Mn@C_{60}$, $Fe@C_{60}$, $Co@C_{60}$ and $Ni@C_{60}$ indicate that there exists hybridization between the C_{60} orbitals and the endoatom orbitals. Also, in these last four endohedral metallofullerenes a split of the threefold degenerate LUMO of C_{60} is observed. The HOMO–LUMO gaps indicate an increase in the chemical reactivity of the endohedral complexes with respect to the pristine fullerene.

Acknowledgements

R.E.E.S. acknowledges the financial support of CONACyT during his Ph.D. studies. A.A.V. is grateful to DGAPA-UNAM for the funding of his scientific projects. Several comments by D. Díaz have been instrumental throughout this work. M.T. Vázquez and S. Jiménez have provided the information requested.

References

[1] S. Guha, K. Nakamoto, Coor. Chem. Rev. 249 (2005) 1111.
[2] H. Shinohara, Rep. Prog. Phys. 63 (2000) 843.
[3] S. Liu, S. Sun, J. Organometallic Chem. 599 (2000) 74.
[4] W. Harneit, Phys. Rev. A 65 (2002) 032322-1.
[5] R.D. Bolskar, A.F. Benedetto, L.O. Husebo, R.E. Price, E.F. Jackson, S. Wallace, L.J. Wilson, J.M. Alford, J. Am. Chem. Soc. 125 (2003) 5471.
[6] R. Tellgmann, N. Krawez, S.H. Lin, I.V. Hertel, E.E.B. Campbell, Nature 382 (1996) 407.
[7] H. Huang, M. Ata, Y. Yoshimoto, Chem. Commun. (2004) 1206.
[8] C. Knapp, N. Weiden, K.P. Dinse, Magn. Reson. Chem. 43 (2005) S199.
[9] B. Elliot, K. Yang, A.M. Rao, H.D. Arman, W.T. Pennington, L. Echegoyen, Chem. Commun. (2007) 2083.
[10] Y.J. Basir, S.L. Anderson, Chem. Phys. Lett. 243 (1995) 45.
[11] T. Pradeep, G.U. Kulkarrii, K.R. Kannan, T.N. Guru Row, C.N.R. Rao, J. Am. Chem. Soc. 114 (1992) 2272.
[12] P. Byszewski, E. Kowalska, R. Diduszko, J. Thermal Anal. 45 (1995) 1205.
[13] G.N. Churilov, O.A. Bayukov, E.A. Petrakovskaya, A.Y. Korets, V.G. Isakova, Y.N. Titarenko, Tech. Phys. 42 (1997) 1111.
[14] P. Reinke, S. Eyhusen, M. Büttner, P. Oelhafen, Appl. Phys. Lett. 84 (2004) 4373.
[15] C.M. Edwards, I.S. Butler, W. Qian, Y. Rubin. J. Mol. Struct. 442 (1998) 169.
[16] M. Avramov-Ivic, L.R. Matija, D. Antonovic, R.O. Loutfy, T. Lowe, P. Rakin, D. Koruga, Trends Adv. Mater. Process. Mater. Sci. Forum 352 (2000) 135.
[17] M. Ivetic, Z. Mojovic, L. Matija, Stud. Adv. Mater. Process. Mater. Sci. Forum 413 (2003) 49.
[18] L.R. Matija, M. Avramov-Ivic, V. Kapetanovic, Contemp. Stud. Adv. Mater. Process. Mater. Sci. Forum 413 (2003) 53.
[19] R.C. Job, Solid Metal-Carbon Matrix of Metallofullerites and Method of Forming Same. U.S. Patent 5288342, 1994. .
[20] B. Delley, J. Chem. Phys. 92 (1990) 508.
[21] B. Delley, J. Chem. Phys. 113 (2000) 7756.
[22] A.D. Becke, Phys. Rev. A 38 (1988) 3098.
[23] J.P. Perdew, Y. Wang, Phys. Rev. B 45 (1992) 13244.
[24] W. Koch, M.C. Holthausen, A Chemist's Guide to Density Functional Theory, Wiley-VCH, Weinheim, 2001.
[25] M. Marlo, V. Milman, Phys. Rev. B 62 (2000) 2899.
[26] S. Tsuzuki, H.P. Lüthi, J. Chem. Phys. 114 (2001) 3949.
[27] M. Filatov, D. Cremer, J. Chem. Phys. 123 (2005) 124101.
[28] M. Panavello, A.F. Jalbout, B. Trzaskowski, L. Adamowicz, Chem. Phys. Lett. 442 (2007) 339.
[29] R.S. Mulliken, J. Chem. Phys. 23 (1955) 1833.
[30] F.L. Hirshfeld, Theor. Chim. Acta B 44 (1977) 129.
[31] F. De Prof, C. van Alsenoy, A. Peeters, W. Langenaeker, P. Geerlings, J. Comput. Chem. 23 (2002) 1198.
[32] C. Fonseca-Guerra, J.W. Handgraaf, E.J. Baerends, F.M. Bickelhaupt, J. Comput. Chem. 25 (2004) 189.
[33] P. Balanarayan, S.R. Gadre, J. Chem. Phys. 124 (2006) 204113.
[34] I. Levine, Quantum Chemistry, 5th ed., Prentice Hall, New York, 2000.
[35] E. Kowalska, P. Byszewski, P. Dluzewski, R. Diduszko, Z. Kucharski, J. Alloys Comp. 286 (1999) 297.
[36] C.M. Tang, K.M. Deng, J.L. Yang, X. Wang, Chinese J. Chem. 24 (2006) 1133.
[37] Z. Lin, J. Harris, J. Phys. Condens. Matter 4 (1992) 1055.
[38] S.H. Vosko, L. Wilk, M. Nusair. Can. J. Phys. 58 (1980) 1200.
[39] J. Lu, L. Ge, X. Zhang, X. Zhao, Mod. Phys. Lett. 13 (1999) 97.
[40] J. Lu, W.N. Mei, Y. Gao, X. Zeng, M. Jing, G. Li, R. Sabirianov, Z. Gao, L. You, J. Xu, D. Yu, H. Ye, Chem. Phys. Lett. 425 (2006) 82.
[41] X.Y. Ren, Z.Y. Liu, M.Q. Zhu, K.L. Zheng, J. Mol. Struct. 710 (2004) 175.
[42] M. Chi, P. Han, X. Fang, W. Jia, X. Liu, B. Xu, J. Mol. Struct. 807 (2007) 121.
[43] R. Yamachika, M. Grobis, A. Wachowiak, M.F. Crommie, Science 304 (2004) 281.
[44] J.N. O'Shea, Science 310 (2005) 453.
[45] S. Suzuki, M. Kushida, S. Amamiya, S. Okada, K. Nakao, Chem. Phys. Lett. 327 (2000) 291.
[46] B. Kessler, A. Bringer, S. Cramn, C. Schlebusch, W. Eberhardt, S. Suzuki, Y. Achiba, F. Esch, M. Barnaba, D. Cocco, Phys. Rev. Lett. 79 (1997) 2289.
[47] J. Lu, X. Zhang, X. Zhao, Chem. Phys. Lett. 332 (2000) 51.
[48] J. Lu, X. Zhang, X. Zhao, S. Nagase, K. Kobayashi, Chem. Phys. Lett. 332 (2000) 219.
[49] K. Wang, J. Zhao, S. Yang, L. Chen, Q. Li, B. Wang, S. Yang, J. Yang, J.G. Hou, Q. Zhu, Phys. Rev. Lett. 91 (2003) 185504.
[50] M.S. Dresselhaus, G. Dresselhaus, P.C. Eklund, Science of Fullerenes and Carbon Nanotubes, Academic Press, San Diego, 1996.